

# CLIVAR-GSOP/GODAE Ocean Synthesis Intercomparison Of Global Air-Sea Heat Fluxes Obtained Through Ocean Data Assimilation

Maria Valdivieso, Keith Haines (Univ. Reading), Magdalena Balmaseda (ECMWF), Jennie Waters, Matt Martin (UKMO), Yan Xue (NCEP/NOAA), Andrea Storto (CMCC), Nicolas Ferry (Mercator Ocean), Armin Koehl (Univ. Hamburg), Yosuke Fujii, Takahiro Toyoda (JMA/MRI), You-Soon Chang (GFDL/NOAA), Xiaochun Wang, Tony Lee (JPL/NASA) and Yonghong Yin (BOM)

m.valdiviesodacosta@reading.ac.uk



## Heat Flux Data Sets

15 heat flux products obtained through ocean or coupled data assimilation are examined (Table 1):

- 8 from low-resolution ( $2^\circ - 0.5^\circ$ ) reanalyses (1 - 8),
- 4 of them are eddy-permitting  $\frac{1}{4}^\circ$  reanalyses (9 - 12),
- and the remaining three are coupled reanalyses based on coupled climate models.

	Data Sets	Model	Surface Forcing	Period
1	BOM - PEODAS	MOM2 $2^\circ \times (0.5^\circ - 1.5^\circ)$ 25L	ERA40 until 2002 NCEP-R2 afterwards	1980-2012
2	ECMWF - ORAS4	NEMO $1^\circ \times (0.3^\circ - 1^\circ)$ 42L	ERAi Flux Forcing	1960-2009
3	JMA - MOVECORE	MRI.COM $1^\circ \times (0.3^\circ - 1^\circ)$ 50L	CORE.2	1948-2007
4	JMA - MOVEG2	MRI.COM $1^\circ \times (0.3^\circ - 1^\circ)$ 50L	JRA-25 with Bulk Fluxes	1993-2012
5	Hamburg - GECCO2	MIT $1^\circ \times (0.3^\circ - 1^\circ)$ 50L	NCEP-R1 with Bulk Fluxes	1993-2010
6	JPL - ECCOV4	MIT $1^\circ \times (0.3^\circ - 1^\circ)$ 50L	ERAi + CORE Bulk Forcing	1993-2010
7	NCEP - GODAS	MOM3 $1^\circ \times (0.3^\circ - 1^\circ)$ 40L	NCEP-R2 Flux Forcing	1980-2011
8	CMCC - CGLORS05V3	NEMO $0.5^\circ \times (0.25^\circ - 0.5^\circ)$ 50L	ERAi corr + CORE Bulk Forcing	1990-2011
9	Reading - UR025.3	NEMO v2.3 $1/4^\circ$ 46L	ERAi + CORE Bulk Forcing	1989-2010
10	Reading - UR025.4	NEMO v3.2 $1/4^\circ$ 75L	ERAi + CORE Bulk Forcing	1989-2010
11	Met Office - GloSea5	NEMO v3.2 $1/4^\circ$ 75L	ERAi + CORE Bulk Forcing	1993-2010
12	Mercator - GLORYS2v1	NEMO $1/4^\circ$ 75L	ERAi corr + CORE Bulk Forcing	1993-2009
13	JMA - MOVE-C	MRI.COM $1^\circ \times (0.3^\circ - 1^\circ)$ 50L	Coupled Model Fluxes	1993-2011
14	GFDL - ECDA	CM2.1/MOM4 $1^\circ \times (0.3^\circ - 1^\circ)$ 50L	Coupled Model Fluxes	1993-2011
15	NCEP - CFSR	CFSRv2/MOM4 $0.5^\circ \times (0.25^\circ - 0.5^\circ)$ 40L	CFSR	1980-2011

**Table 1:** Summary of the heat flux products from ocean or coupled reanalyses. Each reanalysis has run with different models and surface forcing fields (third and fourth columns, respectively). The 17-year period (1993 - 2009) is chosen for the flux comparisons based upon the overlapping time frame between products.

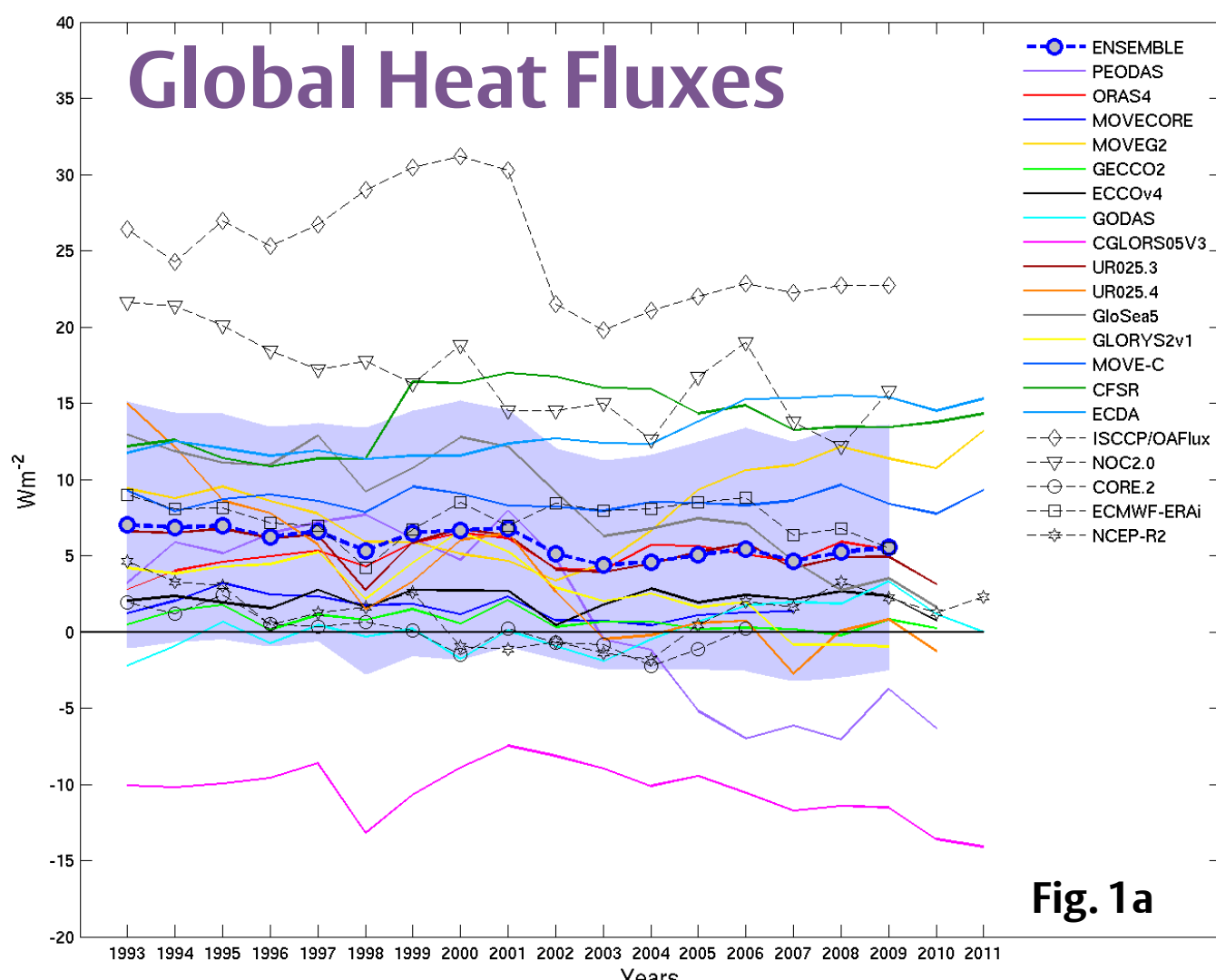


Fig. 1a

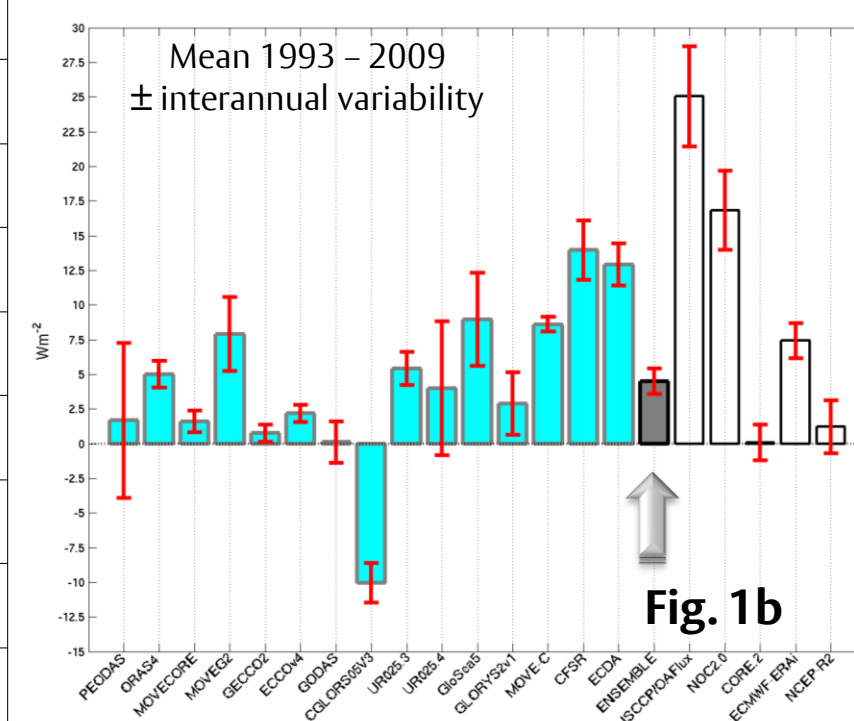


Fig. 1b

Fig. 1b shows time-mean global heat fluxes and their interannual standard deviations over the period 1993 - 2009. The 15-member ensemble mean (grey bar) is  $4.5 \pm 0.92 \text{ Wm}^{-2}$ .

Figure 1a shows the interannual variability of the globally-averaged net surface heat fluxes from ocean/coupled reanalyses compared to independent products, including the combined ISCCP/OAFlux product (Zhang et al., 2004; Yu et al., 2008), the ship-based NOC2.0 product (Berry and Kent, 2009), the Large and Yeager (2009) hybrid flux dataset CORE.2, and 2 atmospheric reanalysis products ECMWF-ERAi and NCEP-R2 - all represented by the light symbols. **Most ocean model products have positive bias (flux into the ocean) although this is often smaller than observational products, e.g., ISCCP/OAFlux and NOC2.0, and smaller than atmospheric reanalyses in some cases. Interannual variations are usually few  $\text{Wm}^{-2}$ , with some exceptions. Coupled Model products (ECDA, CFSR) and CGLORS05V3 appear to be outliers.**

## Ensemble of Flux Estimates

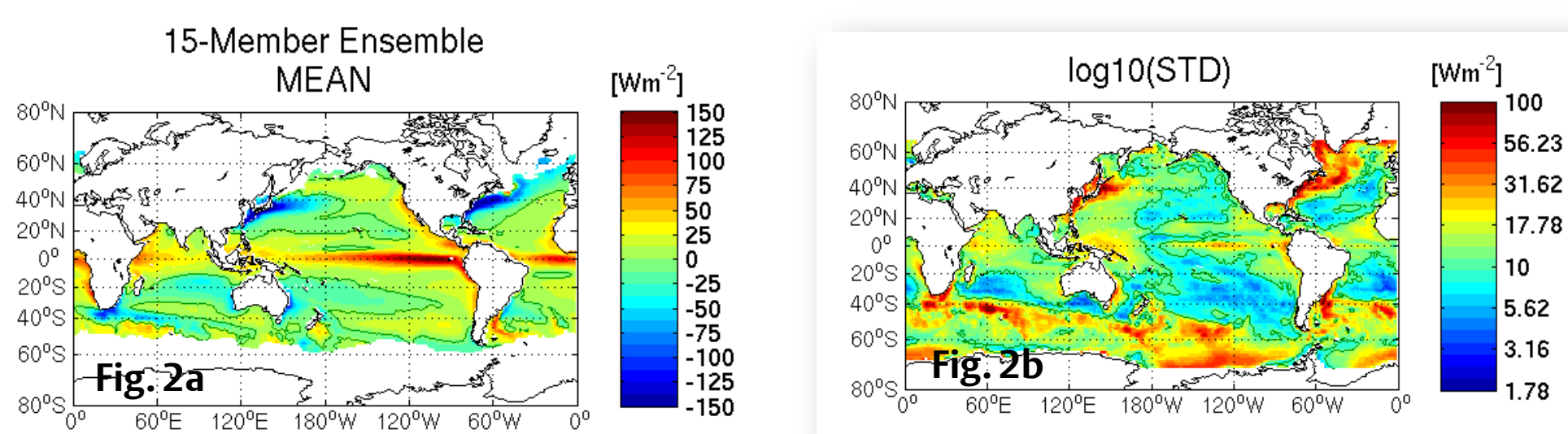


Fig. 2a

Fig. 2b

Figure 2 shows a) the ensemble mean of net surface heat flux estimates based on products in Table 1, and b) its spread (plotted as the logarithm of the STD). The boundary currents and the Southern Ocean are areas of high variability among the heat flux products, while the subtropical gyre interiors have an uncertainty of about  $5-10 \text{ Wm}^{-2}$ , comparable to the global mean spread within the ensemble of  $5 \text{ Wm}^{-2}$  (Fig. 1a).

## Ocean Heat Transports

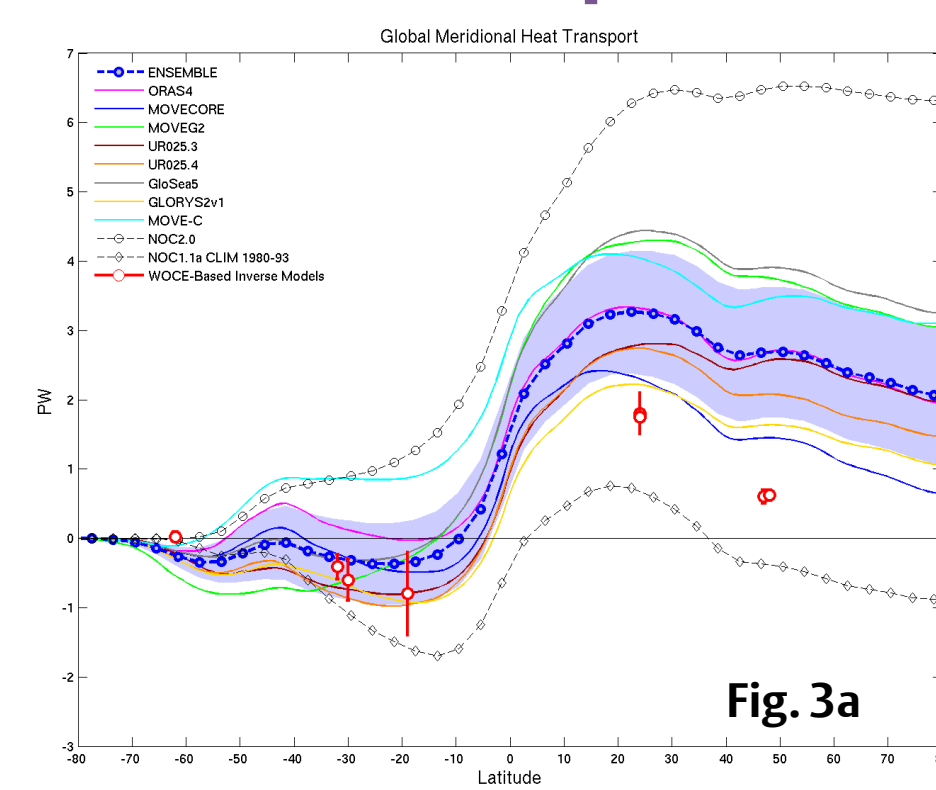


Fig. 3a

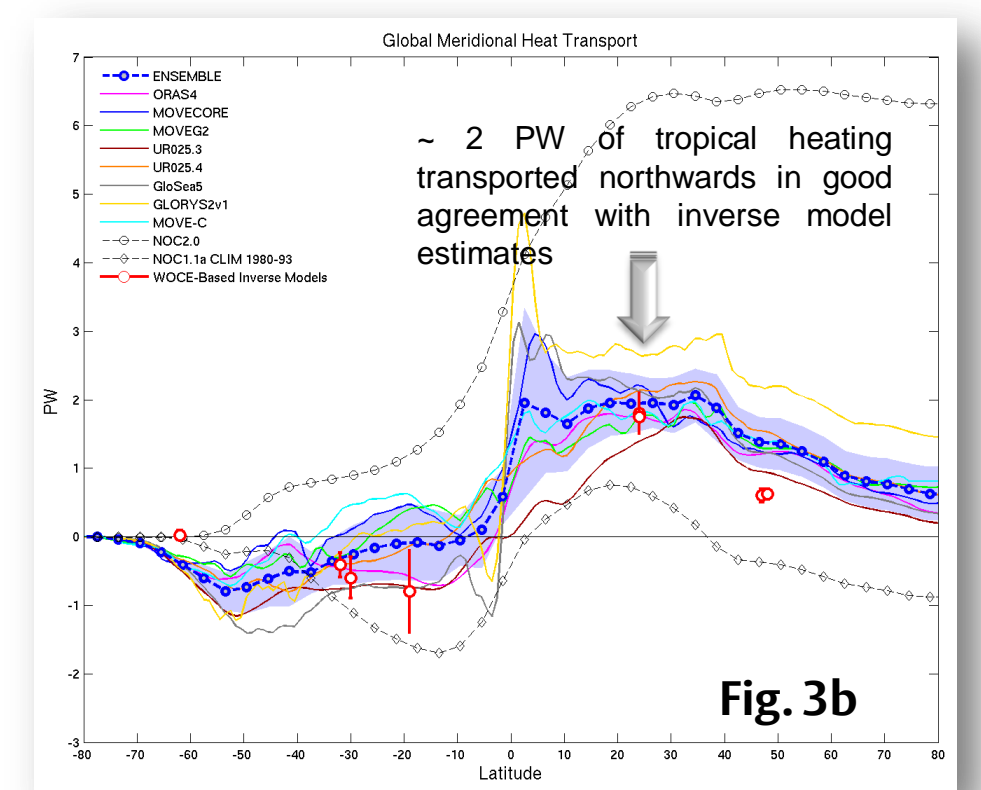


Fig. 3b

Figure 3 shows a) global meridional heat transport inferred from integrated surface heat fluxes and a steady state assumption, and b) from surface fluxes adjusted by assimilation increments. Independent COADS-based heat fluxes (NOC2.0, NOC1.1a) and WOCE-based inverse model estimates at control sections from Ganachaud and Wunsch (2003) and Lumpkin and Speer (2007) are also shown. Assimilation increments improve agreement with external transport estimates and also with mean heat transports estimated directly from reanalysis velocities and temperatures (not shown, Valdivieso et al., 2013).

## Regional Fluxes

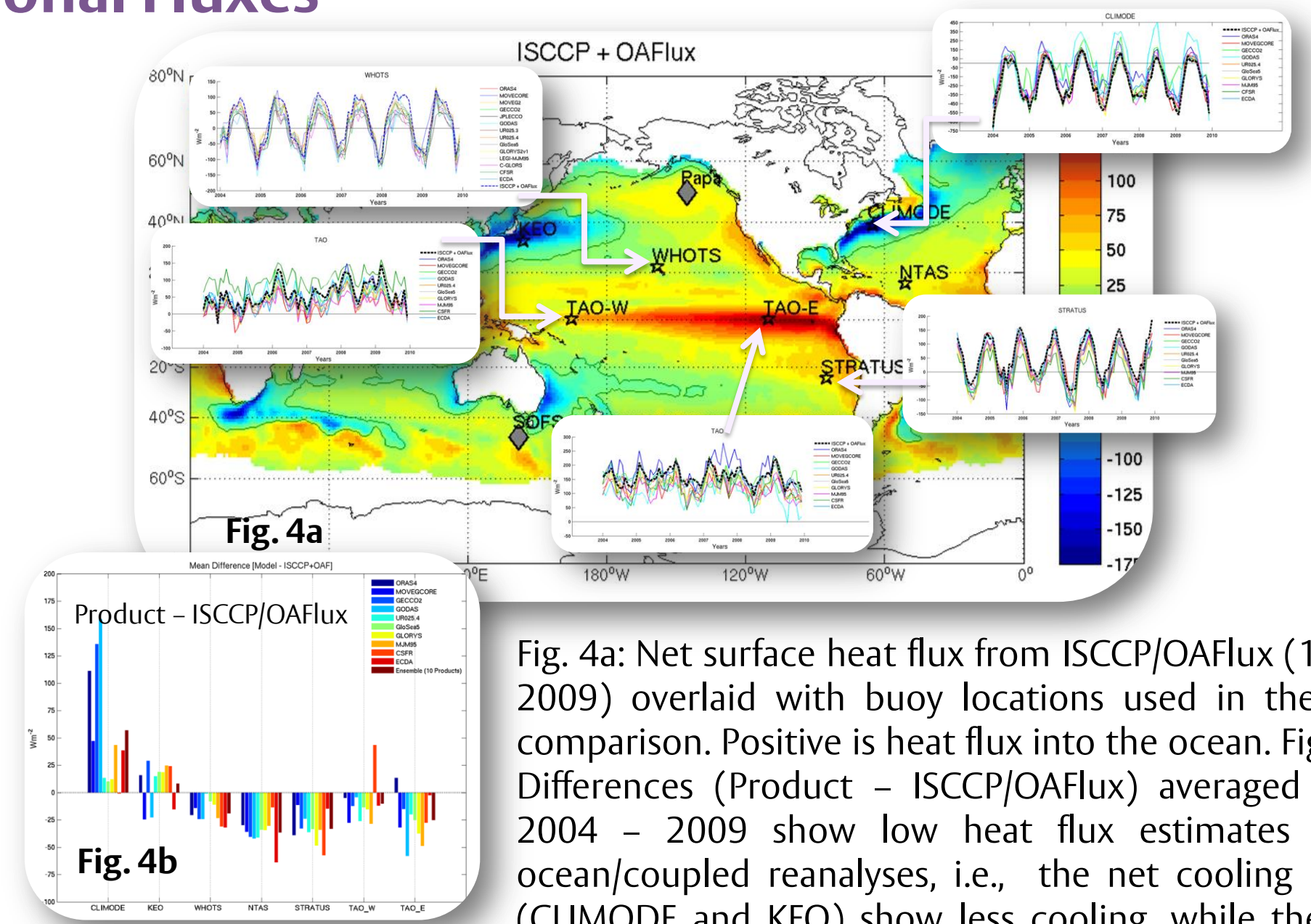


Fig. 4a

Fig. 4b

Fig. 4a: Net surface heat flux from ISCCP/OAFlux (1993-2009) overlaid with buoy locations used in the flux comparison. Positive is heat flux into the ocean. Fig. 4b: Differences (Product - ISCCP/OAFlux) averaged over 2004 - 2009 show low heat flux estimates from ocean/coupled reanalyses, i.e., the net cooling areas (CLIMODE and KEO) show less cooling, while the net heat gain areas (WHOTS, NTAS, STRATUS and TAO) show less warming compared to ISCCP/OAFlux. Variability on seasonal to interannual time scales is generally consistent with ISCCP/OAFlux data (Fig. 4a shows timeseries comparison at some locations).

## Validation Against Flux Measurements

Figure 5 shows a comparison of mean heat flux components from a PIRATA buoy in the Tropical Atlantic ( $10^\circ\text{S}, 10^\circ\text{W}$ ) with flux estimates from various products in Table 1 interpolated to the buoy location.

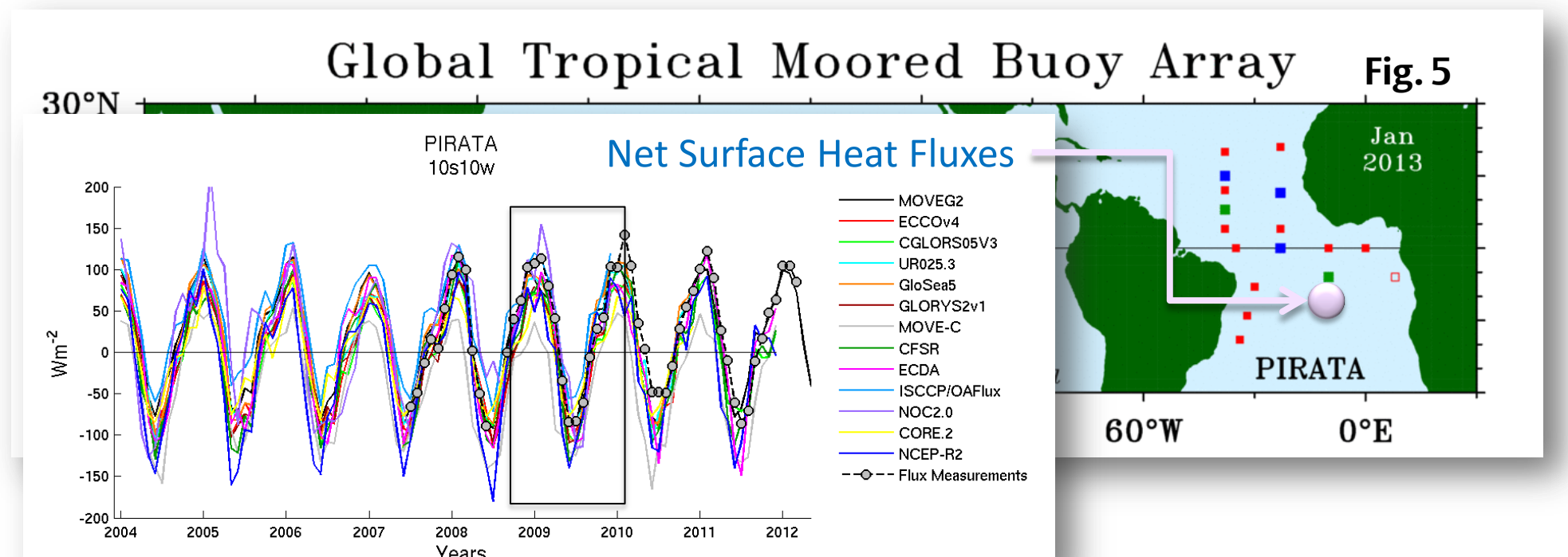


Fig. 5

- Except for the ISCCP/OAFlux, the other net heat flux ( $Q_{\text{net}}$ ) estimates are lower than the buoy mean of  $\sim 28 \text{ Wm}^{-2}$  into the ocean over September 2008 - December 2009 inclusive (16 months)
- Among the ocean reanalysis products, the closest agreement is for MOVEG2, UR025.3 and GloSea5, which show all flux components, as well as the net heat flux, within  $10 \text{ Wm}^{-2}$  of the buoy values

- Global heat flux data sets from ocean /coupled reanalyses have differing global mean closure, although most products have better closure than for observation products alone
- Largest discrepancies among the ocean reanalyses are located around fronts, such as the equatorial tongue, the western boundary currents and the ACC
- Even small global flux imbalances imply large heat transport discrepancies with observations. When reanalysis fluxes are adjusted by data assimilation increments the implied meridional transports agree well with hydrographic transport estimates
- Regional reanalysis heat flux variability is in good agreement with OAFlux/ISCCP data. At most buoy locations reanalyses show lower fluxes by  $20-40 \text{ Wm}^{-2}$ , consistent with global bias in OAFlux/ISCCP, except in cooling areas near western boundary buoys, KEO and CLIMODE.
- Ongoing work is evaluating reanalysis heat flux components against in situ flux measurements from the OceanSITES project <http://www.pmel.noaa.gov/tao/oceansites/flu>